

1 Introduction to Hall Effect Thrusters

1.1 Hall Effect Thruster Operation

A Hall Effect Thruster (HET) is a type of electric propulsion that uses both electromagnetic and electrostatic forces to operate. It is made up of the following components: an acceleration chamber, magnetic coils (or a permanent magnet), an anode and gas injector at the beginning of the acceleration chamber, and an external cathode. An example of which can be seen in Figure 1.

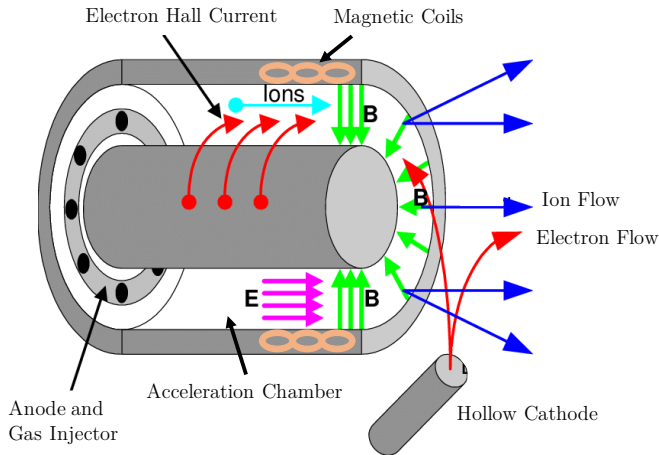


Figure 1: A typical HET: magnetic field lines are shown in green and electric field lines are shown in purple [1].

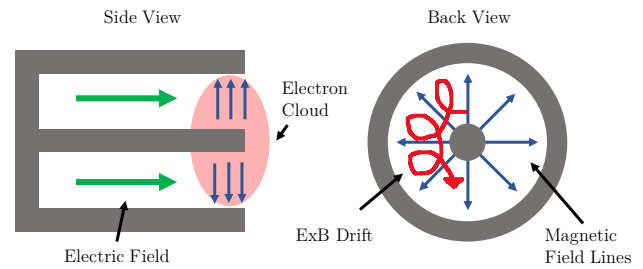


Figure 2: Diagram showing magnetic and electric field lines, electron positions, and ExB drift in a typical HET.

As the Cathode is heated it emits electrons. Some of these are attracted towards the anode and reach the radial magnetic field in the thruster. At this point the electrons get trapped in an ExB drift due to the combination of an electric and a magnetic field (see in Figure 2). The electrons are prevented from reaching the anode by the Hall Effect: as the electrons move towards the anode, they generate a Hall current which produces a Lorentz force acting in the opposite direction. This force is similar to the electrostatic force pulling the electrons towards the anode. Hence, the electrons remain in equilibrium at the end of the thruster and build up over time. An electric field is generated as there is a potential difference between the electron cloud and the thruster anode. The electric field generated by the build-up of electrons is what accelerates the propellant. Some electrons emitted by the cathode do not get attracted to the anode. These combine with positive ions in the downstream plume. This neutralizes the system and prevents the build-up of charge on a spacecraft.

The gas injector periodically releases an inert gas (usually Xenon) into the acceleration chamber. Drifting gas particles collide with electrons in the chamber which can cause them to become positive ions. The ions can then be accelerated out of the acceleration chamber by the electron-generated axial electric field. The ions reach a high speed and are then ejected from the thruster in the axial direction. The change in momentum from ejected ions is how a HET generates thrust [2].

1.2 Cylindrical Hall Thrusters

A Cylindrical Hall Thruster (CHT) is a plasma thruster like a HET, however they have a lower surface-to-volume ratio than conventional HETs and, thus, are more promising for scaling down [3]. This makes them ideal for use on very small spacecraft. Like a HET, a CHT uses an axial electric field to accelerate ionized propellant. It also generates the axial electric field in the same way: through trapping electrons at the end of the thruster. The difference between a typical HET and a CHT comes in how the electrons are trapped: typical HET's use a radial magnetic field in combination with an axial electric field to trap electrons in an ExB drift. A CHT on the other hand, traps electrons using a magnetic mirror: to achieve this, electromagnets are used to generate a varying magnetic field. This means trapped electrons in a CHT bounce back and forth radially, whereas in a typical HET, electrons circle about end of the thruster in an ExB drift.

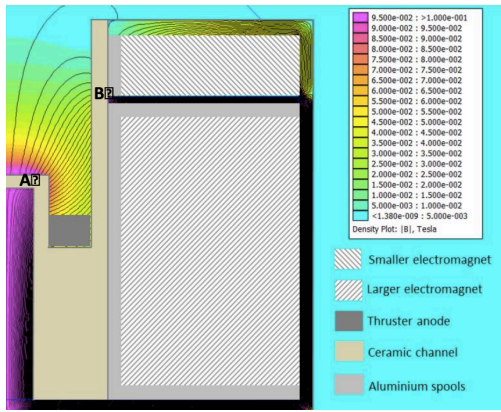


Figure 3: The CHT used. The varying magnetic field can be interpreted with the key on the right [4].

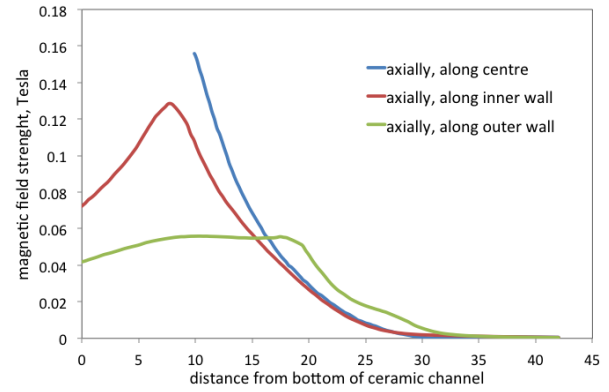


Figure 4: Magnetic field strength along the three axial paths in the CHT tested [4].

The CHT magnetic mirror can be seen in Figure 3 and is situated between points A and B. A magnetic mirror works because electrons approximately follow magnetic field lines, at points where the magnetic field is strong the electrons can change direction and are essentially “reflected”: this is what occurs at points A and B. Electrons trapped in the magnetic mirror create a negative potential which accelerates ions in the plasma out of the thruster in the axial direction. This is how a CHT generates thrust.

1.3 Hall Thruster Applications

HETs were originally used for station keeping and were almost always a form of secondary propulsion. This was because they were limited by poor power systems in the past which could not reliably supply the power needed. Since the turn of the century, HETS have been more commonly used as a primary propulsion.

HETs are a popular choice for orbit raising to Geostationary Earth Orbit (GEO) and Medium Earth Orbit (MEO) as they offer a significantly reduced weight compared to chemical based systems. This is because they have a much higher specific impulse (I_{sp}). Although Gridded Ion Thrusters also have a very high I_{sp} , HETs provide a high enough thrust to reach target orbits in a reasonable time – which also saves money as operators can get more time out of their spacecrafts. A high thrust density means HETS are well suited to movement of very high mass spacecraft, making them a common choice for high mass spacecraft stabilization.

HETs today have many industrial applications. These range from orbit raising, to interplanetary transfers. To list a few examples: all Airbus Defence and Space satellites (most of which have a GEO orbit), the ESA Smart-1 mission to the Moon, the interplanetary NASA Psyche mission, The ESA Inmarsat-6 GEO based communications satellite, and the NASA Asteroid Redirect Mission [5].

1.4 Advantages and Disadvantages

HETs have the big advantage of having the highest thrust for an electric propulsion system with an I_{sp} as high as 2000 seconds. They are also not as complex as GITs to manufacture as they do not require a specially made grid. HETs are at a disadvantage however, because they have a lower efficiency compared to GITs. This is because ions may leave a HET at various angles, and there is little that can be done to prevent this (other than to increase the exhaust velocity). GITs designed so the exhaust plume is as collimated as possible which allows for much higher I_{sp} s. Another disadvantage of HETs is they are very susceptible to erosion. Electrons and ions alike collide very easily with the walls at the end of the thruster and over time can cause the thruster to stop working altogether. This is especially a problem if the magnetic field intersects the thruster wall, which can only be mitigated with a very well-designed thruster.

2 Theoretical Calculations

Charged particles in a magnetic field undergo circular motion. The Larmor Radius is the radius of that circle and the cyclotron frequency is the rate at which the particles complete the circle. It is important to find the Larmor Radius for both electrons and ions as they both heavily effect CHT performance. These are calculated as follows:

$$\text{cyclotron frequency} = \omega_c = \frac{q\vec{B}}{m} \quad \text{Larmor Radius} = r_L = \frac{mv_{\perp}}{q\vec{B}}$$

Particle	Magnetic Field Strength (T)	Beam Voltage (V)	Cyclotron Frequency (Hz)	Larmor Radius (m)
Ion at B _{min} , V _{b_max}	0.015	226.5	1.64x10 ⁴	1.335
Ion at B _{max} , V _{b_min}	0.160	84.5	1.75x10 ⁵	0.078
Electron at B _{max}	0.015	-	2.63x10 ⁹	8.03x10 ⁻⁴
Electron at B _{min}	0.160	-	2.81x10 ¹⁰	7.53x10 ⁻⁵

Table 1: cyclotron frequency and Larmor Radius at best and worst conditions for electrons and ions in the CHT.

Table 1 shows the completed theoretical calculations for the maximum and minimum possible Larmor Radius for ions and electrons. These are shown with the Cyclotron Frequencies for each. The maximum and minimum magnetic field strength were determined by using values from Figure 3 and Figure 4. The maximum and minimum beam voltages found using the maximum and minimum anode voltages seen in the lab (206.5 V and 64.5 V respectively) and using the following equation:

$$V_b = V_{anode} - (V_{plasma} + V_{cathode})$$

For electrons, it is important to minimize the Larmor Radius, so they can easily follow magnetic field lines without colliding with the CHT wall. Without space to circulate, an electron cloud could not build up, removing the CHTs potential generate thrust. Hence the electron Larmor Radius must be much less than the CHT depth. The calculations in Table 1 show the worst-case electron Larmor Radius to be 0.803 mm. In comparison, the CHT depth is 39 mm. which almost 50 times greater. This is an acceptable margin and increases confidence in the operation of the CHT.

$$r_{Lelectronideal} \ll L$$

For ions, it is important to maximize the Larmor Radius as curvature in the ion path can cause them to leave the CHT at an angle to the axial path, which reduces thrust. In a worst-case scenario, too small a Larmor Radius could cause ions to curve too much and not leave the CHT at all, preventing thrust generation. Hence, the ion Larmor Radius must be much greater than the CHT depth. The calculations in Table 1 show the worst-case ion Larmor Radius to be 78 mm. This is very close to the CHT depth of 39 mm, which is bad. This means ions at the worse-case region curve a lot, leaving the CHT at a very high angle, or even not at all. This greatly reduces efficiency. For ions on the wall of the thruster (best case scenario), the Larmor Radius can be as high as 1.335 m, which is about 34 times greater than the CHT depth. Ions here will still curve, but at an acceptable level. Combined, this information reduces confidence in the CHTs efficiency.

$$r_{Lionideal} \gg L$$

This shows the CHT could probably be made more efficient by reducing the magnetic field strength as it would increase the electron Larmor Radius and decrease the ion Larmor Radius. Although it would be bad to increase the electron Larmor Radius, it has room to be increased, whereas the ion Larmor Radius is far too similar to the CHT depth.

3 Experimental Calculations

The following calculations were completed for all data points in lab seven. Lab seven was split into two halves and the constants were slightly different in each half. Here I explain the calculation process without showing the calculated values, however for a better understanding, please see the full calculations which I have made available online [6].

3.1 Specific Impulse

For each operating point, the specific impulse can be calculated with $I_{sp} = \frac{\alpha \eta_{cos} \eta_m}{g_0} \sqrt{\frac{2qV_b}{M_{ion}}}$. Specific impulse shows how effectively a rocket uses fuel. In this equation, g_0 , q , and M_{ion} are known fundamental parameters, and η_m is given. The value α refers to the losses due to the doubly charged ions, which is determined by: $\alpha = \frac{1 + \frac{I^{++}}{\sqrt{2} I^+}}{1 + \frac{I^{++}}{I^+}}$. In this equation, I^{++} is the doubly charged ion current and I^+ is the charged ion current. The proportion of doubly charged ions, n^{++}/n_{total} , is 0.2. The current from double charged ions is double which needed to be taken into account. Therefore, the ratio of currents was found with: $\frac{I^{++}}{I^+} = 2 * \frac{n^{++}}{n_{total}} * \frac{n_{total}}{n^+} = 0.50$. This gave α to be 0.902. The next unknown was η_{cos} (the loss due to beam divergence), this was found with the following formula: $\eta_{cos} = (1 + \cos^2(\theta))/2 = 0.88$. This left only V_b (beam voltage) to be determined. One problem with Hall Thrusters is V_b varies and is not directly controlled. Thus, it has to be estimated. This is done with the following formula: $V_{beam} = V_{anode} - (V_{plasma} + V_{cathode})$. For every data point, the anode voltage was unique, as well as this, the cathode voltage was different for each lab. The plasma voltage was given to be 10 V. By plugging these values into the equation for I_{sp} , values for each data point were found (see Table 2 for examples).

	Laser Data Number	1	2	...	37
	ydiff (mm)	2.52E-03	3.29E-03	...	0.012827
	Lab Half	1	1	...	2
	Anode Voltage (V)	81.1	80.1	...	89.5
	Anode Current (A)	0.63	0.63	...	2.32
	Anode Power (W)	51.3	50.7	...	207
	Beam Voltage (V)	24.1	23.1	...	29.3
	Beam Current (A)	0.487	0.487	...	1.783
	Specific Impulse (s)	515	504	...	568
	Thrust from Anode Current (N)	2.55E-03	2.50E-03	...	1.03E-02
	Thrust from I _{sp} (N)	3.15E-03	3.08E-03	...	4.16E-03
	Experimental Thrust (N)	7.12E-04	9.31E-04	...	3.63E-03
Thrust from Anode Current	Anode Efficiency (%)	10.18	9.88	...	34.19
	Total Efficiency (%)	5.02	4.84	...	26.83
Thrust from Isp	Anode Efficiency (%)	15.48	15.02	...	5.59
	Total Efficiency (%)	7.63	7.36	...	4.39
Thrust from Balance	Anode Efficiency (%)	0.79	1.37	...	4.25
	Total Efficiency (%)	0.39	0.67	...	3.33

Table 2: A excerpt from a full excel sheet calculating all of the values on the left for every power sweep from 1 to 37, by missing out a test power sweep 19, 36 columns of data were processed. Many of these are plotted in Section 4.

3.2 Thrust Calculations

For each operating point, thrust can be calculated in one of three ways: using the direct thrust balance measurements, using the anode voltage and current, or using the anode voltage and mass flow rates. The thrust from the balance was

found by multiplying the force balance y-axis difference by a calibration factor: $T_{balance} = \Delta y * 0.2828$. The thrust from the anode current was found using the following formula: $T_1 = \alpha \eta_{cos} \sqrt{\frac{2M_{ion}}{e}} I_b \sqrt{V_b}$. The only unknown here was the beam current. This was found by taking the beam current efficiency and multiplying it with the anode current: $I_b = \eta_b * I_{anode}$. Finally the thrust from anode voltage and mass flow rate (I_{sp} thrust) was be found by multiplying the specific impulse for each data point by the mass flow rate (which varied per lab) and gravity: $T_2 = \dot{m} I_{sp} g_0$. Each of these was calculated for every data point as seen in the sample provided of Table 2.

3.3 Efficiency Calculations

The anode and total efficiencies were calculated for each operating point. The anode efficiency was calculated with the following formula: $\eta_{anode} = \frac{T^2}{2\dot{m}_{anode} P_{anode}}$. The only unknown here was P_{anode} which is simply the anode voltage times the anode current. The mass flow rate of the anode had to be given in kilograms per second which required a simple conversion. The total efficiency was calculated with the following formula: $\eta_{total} = \frac{T^2}{2(\dot{m}_{anode} + \dot{m}_{cathode})(P_{anode} + P_{cathode} + P_{electromagnets})}$. The power of the cathode and electromagnets changed between labs but were a set value throughout each. The mass flow rate for the cathode was also given. The power of the cathode was calculated by multiplying the cathode voltage and cathode current. The total electromagnet power was determined by summing the power output of all the magnets used. These efficiencies were calculated for all thrust types and data points as seen by the sample in Table 2. As expected, the experimental thrust from the balance was lower than the theoretically calculated thrusts – this is usually the case because it is near impossible to account for all inefficiencies. A summary of all this data is nicely visualized in Figure 10.

4 Analysis

4.1 Discussion of Plotted Data

For the analysis, data was used from both halves of lab 7. These labs had different anode flow rates, cathode powers, and electromagnetic powers. Rather than label graphs with the unique properties, the graphs were labelled with either “Lab 1” or “Lab 2” to indicate the data set referred to, please see Table 3.

Parameter	Lab 1 Value	Lab 2 Value
Cathode Flow Rate (sccm)	8	8
Anode Flow Rate (sccm)	10	12
Cathode Power (W)	51.23	54.87
Electromagnetic Power (W)	1.52	1.90

Table 3: The values used in each lab half.

As seen in Table 3, the lab 2 data had a higher anode flow rate, a higher cathode power, and a higher electromagnetic power. For reasons discussed in Section 2, a higher electromagnetic power would likely decrease the efficiency of the CHT. Considering the increase in the cathode power was only 3 W (a 7 % increase), which is very small considering the anode power operated up to 200 W, it is unlikely that much change is because of the cathode power change. Hence, for observed improvements in the CHT performance in the following figures, it can be expected that these come almost exclusively from the change in anode mass flow rate, which went from a value of 10 to 12.

Figure 6 shows the anode current against anode voltage. It can be seen that for both sets of data, the anode current increased with anode voltage. This is not ideal as in a perfect CHT the anode voltage and current are independent. It is bad to have a varying current with voltage because for the same power input, a CHT with a higher current has a lower potential different through which ions are accelerated (since $P = IV$). Both sets of data show the current increasing and then flattening out. This shows that the CHT gets better at being more efficient at higher anode voltages. The lab 2 data plot shows a higher anode current for the same anode voltage compared to the lab 1 data. This affirms the validity of the

data and is to be expected because the anode mass flow rate is higher for lab 2 (12 compared to 10). Higher mass flow rate produces a higher current because the ions carry the current, so more ions means more current.

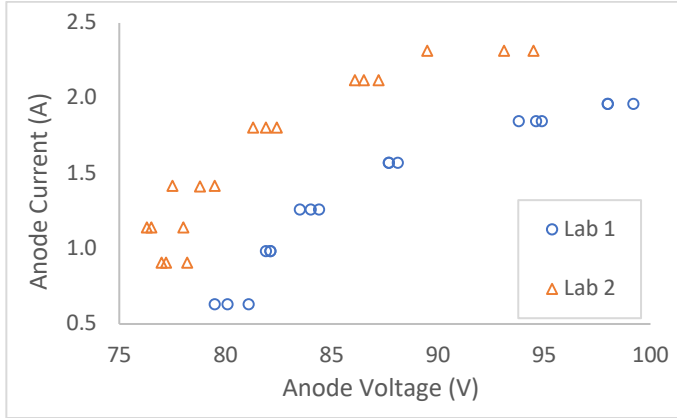


Figure 6: Anode current plotted against anode voltage for both lab conditions.

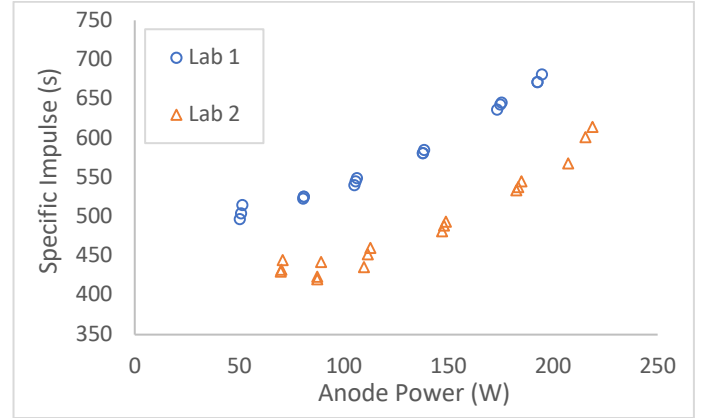


Figure 7: Specific impulse plotted against anode power for both lab conditions.

In Figure 7, it can be seen that for an increasing anode power, there is an increased specific impulse. This is expected since I_{sp} for Hall Thrusters is directly proportional to the square root of the beam voltage ($I_{sp} \propto \sqrt{V_b}$). Beam voltage is a summation which includes anode voltage which increases with the anode power. The maximum I_{sp} recorded was 681 seconds: this is a high I_{sp} and yet is still quite low for a HET (the usual values can be near to 1100 seconds [7]). This may be so low due to a low Larmor Radius for the ions or simply other inefficiencies adding up. The lab 2 data had a lower I_{sp} for the same anode power. This was to be expected because I_{sp} is inversely proportional to mass flow rate, so for an increased mass flow rate, it is expected to see a decreased I_{sp} . The lab 2 data has an increased mass flow rate, so this relationship increases confidence in the data accuracy.

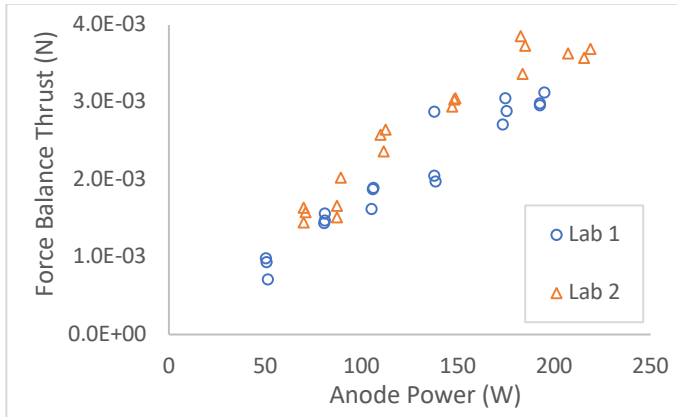


Figure 8: Thrust (from force balance) against anode power.

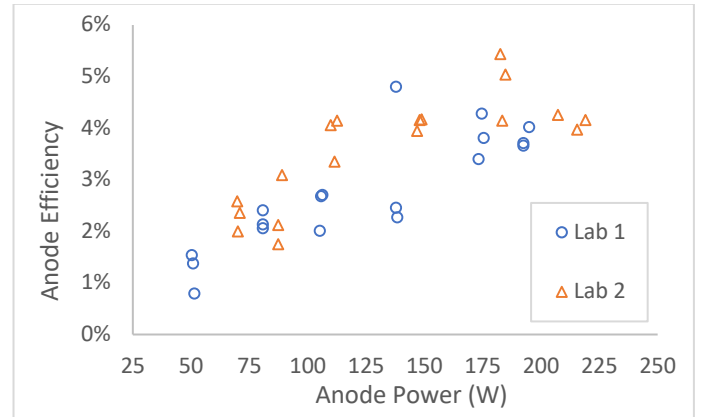


Figure 9: Specific impulse against anode power (using thrust from force balance) for both lab conditions.

Figure 8 shows a positive and linear relationship between the thrust from the force balance and the anode power. This shows that a higher power can be used to achieve a higher thrust. This makes sense because, thrust is proportional to the beam current times the square root of the beam voltage ($T \propto I_b \sqrt{V_b}$). Hence as power increases, so should the thrust. The highest thrust achieved was 3.85 mN which is an acceptable thrust for a hall thruster of this size [8]. The lab 2 and lab 1 data were both very similar except the lab 2 data produced a slightly higher thrust for the same anode power. This was expected as the lab 2 data had a higher mass flow rate of ions, which is directly proportional to thrust ($T \propto \dot{m}$).

Figure 9 shows the variation of anode efficiency against anode power. This data is more scattered than the other graphs which makes sense because anode efficiency is proportional to thrust squared ($\eta_{anode} \propto T^2$). Therefore, errors in the thrust calculation are compounded. Despite the scatter, it can still be seen that anode efficiency increases with anode power. This shows that the thruster operates better at higher anode powers. As well as this, it can be seen that the lab 2 data had a

slightly higher anode efficiency for the same anode power. This is likely because the lab 2 data had a slightly higher thrust for the same anode power, the reasons for which are discussed in the analysis of Figure 8.

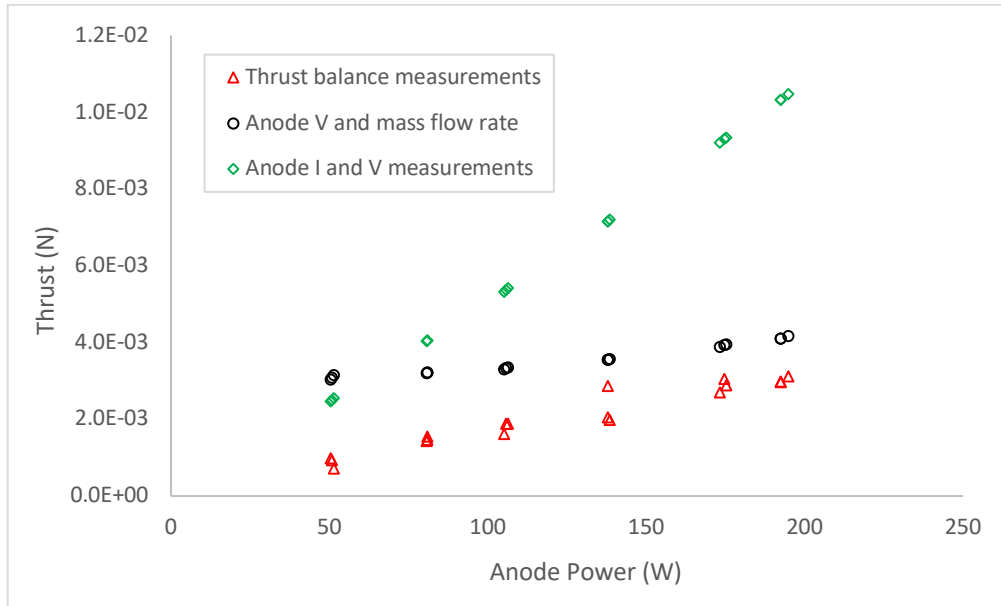


Figure 10: Thrust against anode power for the three different methods of measuring thrust. This graph used data from lab 1 only. This figure can be used to visualize most of the calculated data from the lab.

Figure 10 shows that the three different methods for calculating results, give different results for the same anode power. The method using anode voltage and current has large differences in magnitude and gradient compared to the experimental results: this is not a good way to calculate thrust. This is likely because both beam voltage and beam current are used which both have to be approximated for HETs. The differences between the other two methods are likely because some efficiencies were off, the beam voltage or other minor inefficiencies. Of the two methods that do not directly measure thrust, the method using the I_{sp} was clearly better as it was much more similar to the directly measured thrust for varying anode powers. As well as this, it tended towards the same values as the efficiency from the thrust balance measurements at higher anode powers. This is likely because the smaller efficiencies had less of an effect when the thruster is running at full power, causing them to become insignificant. For all cases, the thrust increased with anode power. This was expected as more power means a higher the potential difference which ions are accelerated across which means greater thrust.

4.2 Further Discussion

The analytical methods for calculating would be more accurate for a GIT for two reasons. Firstly, in a GIT, the ions begin accelerating at the same place (within the Debye Length of the first grid) and then have a controlled acceleration against a known and carefully controlled potential. In a HET on the other hand, inert gas is accelerated from wherever it is ionized which varies, this leaving the average acceleration distance and beam potential unknown. In other words, the beam current and voltage are known for a GIT, whereas in a HET, they are not. These are necessary for an accurate calculation. That said, Langmuir probes can be used in a HET to measure the beam current. The second reason is that GITs are designed so the exhaust plume is as collimated as possible. In a HET, the exhaust plume has a wide beam angle which is difficult to estimate. These two reasons combined make clear why the equations for thrust would be more accurate for a GIT.

This beam voltage likely strongly affects the results collected because it has to be approximated. Beam voltage is approximated by the discharge voltage (anode voltage) minus the summed plasma and cathode voltage. The reason the beam voltage is often inaccurate is because the plasma and cathode voltages are hard to measure. Figure 10 shows that the thrust from I_{sp} was slightly higher than the measured thrust. Since this calculation is proportional to the square root of beam voltage, it suggests that the beam voltage used in the labs was approximated too high. This is backed up by looking at the thrust from the anode voltage and current which is proportional to the square root of beam voltage too, this plot also ran above the experimental calculations. It's likely that the beam current approximation (estimated using an

efficiency factor) was also too high because the gradient was greater than the experiment result. This suggests the estimated plasma voltage, or the cathode voltage was too low, and thus, the plasma voltage in the thruster was potentially too high.

The experimental results show that despite the fact that the CHT is designed to best operate at an anode power of 50 – 200 W, it actually worked best the highest anode power tested of 200 W. Unfortunately, the CHT cannot operate at much higher power ranges as it is limited by material selection (it starts to melt at > 250 W). The CHT could be improved by rebuilding it with higher melting point materials and running it at higher powers to find an optimum.

Method of Calculating Thrust	Standard Deviation of Averages (N)
Using Anode Current	1.00x10 ⁻⁴
Using I _{sp}	5.56x10 ⁻⁵
From Force Balance	1.66x10 ⁻⁴

Table 4: the standard deviation of data averages for each method of calculating thrust.

The data was good because each voltage and current variation was measured three times. This allowed an average to be calculated for every set of conditions. Table 4 shows the average standard deviation for each thrust measurement. All the average standard deviations were much smaller than the magnitude of the data (0.1s of millinewtons compared to 1s millinewtons) which increases confidence 3 data points were sufficient per average. Notably, the calculations using I_{sp} had much smaller variations than the calculations using anode current which suggests that anode current played a role in making the data noisier. The thrust balance measurements were limited as the calculated the y-axis difference relied on judging by eye where exactly the thruster cut off. This was sub-optimal as human error was introduced. Ideally, the points at which the thruster turned off could have been recorded and mapped onto the thrust balance data automatically. This would've taken out the element of human error.

5 Conclusion

Throughout the lab we showed that the CHT works and produces a reasonable amount of thrust (in the order of millinewtons). The I_{sp} observed was not spectacularly high with a maximum of 681 seconds. For a CHT of the same size, an I_{sp} of about 1100 seconds is expected [7]. The highest total efficiency recorded was 4.15 %. For a normal HET, the total efficiency is expected to be about 6 % to 30 % at 100 W to 200 W [8]. This shows that this thruster was very inefficient. The main reason the CHT did not operate at a higher I_{sp} and efficiency is likely because the Larmor Radius for ions was very low: only being about double the CHT depth in some areas. The data collected clearly showed that for higher anode power and higher anode mass flow rate, the efficiency of the thruster can be improved. Because of this, these two factors should be maximized on any future iterations of the thruster.

The CHT studied is being considered for orbit raising small satellite constellations from 500 km to 1100 km. By making assumptions about the mass of the satellite, the fuel mass required for this can be calculated by rearranging the rocket equation: $m_f = m_s e^{\frac{\Delta V}{V_e}} - m_s$. The change in velocity (ΔV) required for a spacecraft to move from one circular orbit to another is found by considering a Hohmann transfer (a Hohmann transfer is the theoretically most efficient transfer [9]). By using the average I_{sp} of 600 seconds, the ΔV comes out to be 120.2 m/s. The exhaust velocity for the CHT can be found using the following equation: $V_e = I_{sp} * g_0 = 5886$ m/s. Now, for a satellite weighing 10 kg, this gives the mass of fuel to be 0.206 kg. This is only 2% additional weight which is a very good fuel mass fraction. This number increases to 3.8% for a doubled velocity change required which is also very good. This shows that even though the CHT tested is very inefficient and has a low I_{sp} compared to others, it is still a hall thruster with a high I_{sp} compared to chemical systems. Therefore, the CHT studied would work fine for this satellite mission, even though it can be made more efficient.

Compared to other similar sized HETs and Cusped Field Thrusters (CFT), the CHT studied had a very low efficiency. At MIT a CFT was tested which achieved an efficiency of 44.5 % [10]. Also, as stated before, generic HETs are tested with efficiencies up to 30 %. This shows that the CHT tested could be improved and optimized. This may be achieved by implementing some of the recommended improvements made in this report.

6 Bibliography

- [1] Ashkenazy, Joseph & Appelbaum, G & Ram-Cohen, T & Warshavsky, A & Tidhar, I & Rabinovich, L. (2007). VENUS Technological Payload - The Israeli Hall Effect Thruster Electric Propulsion System. 10.13140/2.1.4172.4801.
- [2] A. D. Gallimore and A. F. Thurnau, "The physics of spacecraft hall-effect thrusters", 2008.
- [3] Ryan, Charlie, University of Southampton, SESA6071 Spacecraft Propulsion Lecture Slides.
- [4] A. Smirnov, Y. Raitses and N. Fisch, "Experimental and theoretical studies of cylindrical Hall thrusters", Physics of Plasmas, vol. 14, no. 5, p. 057106, 2007. Available: 10.1063/1.2718522.
- [5] D. Lev, "Performance Validation and Plume Divergence of the CAM200 Low Power Hall Thruster", Aeronautics and Aerospace Open Access Journal, vol. 2, no. 2, 2018. Available: 10.15406/aaaj.2018.02.00033.
- [6] J. Sivyer, "CodingWithJack/Spacecraft-Propulsion-Lab", GitHub, 2019. [Online]. Available: <https://github.com/CodingWithJack/Spacecraft-Propulsion-Lab>. [Accessed: 12- Dec- 2019].
- [7] D. Lev, "Performance Validation and Plume Divergence of the CAM200 Low Power Hall Thruster", Aeronautics and Aerospace Open Access Journal, vol. 2, no. 2, 2018. Available: 10.15406/aaaj.2018.02.00033.
- [8] Y. Raitses, A. Smirnov and N. Fisch, "Cylindrical Hall Thrusters", 37th AIAA Plasmadynamics and Lasers Conference, 2006. Available: 10.2514/6.2006-3245 [Accessed 12 December 2019].
- [9] A. Miele, M. Ciarci and J. Mathwig, "Reflections on the Hohmann Transfer", Journal of Optimization Theory and Applications, vol. 123, no. 2, pp. 233-253, 2004. Available: 10.1007/s10957-004-5147-z.
- [10] D. Courtney and M. Mart`mez-S`anchez, "Diverging Cusped-Field Hall Thruster (DCHT)", Erps.spacegrant.org, 2019. [Online]. Available: https://erps.spacegrant.org/uploads/images/images/iepc_articledownload__1988-2007/2007index/IEPC-2007-039.pdf. [Accessed: 12- Dec- 2019].